The, R., & Hasselbach, W. (1977) *Eur. J. Biochem. 24*, 611.
Thomas, D. D. (1978) *Biophys. J. 24*, 439.
Thomas, D. D., & Hidalgo, C. (1978) *Proc. Natl. Acad. Sci. U.S.A. 75*, 5488.
Verjovski-Almeida, S. (1981) *J. Biol. Chem. 256*, 2662.
Verjovski-Almeida, S., & Inesi, G. (1979) *J. Biol. Chem. 254*, 18.
Verjovski-Almeida, S., Kurzmack, M., & Inesi, G. (1978) *Biochemistry 17*, 5006.
Watanabe, T., & Inesi, G. (1982) *Biochemistry 21*, 3254.
Watanabe, T., Lewis, D., Nakamoto, R., Kurzmack, M., Fronticelli, C., & Inesi, G. (1981) *Biochemistry 20*, 6617.
Yamamoto, T., & Tonomura, Y. (1967) *J. Biochem. (Tokyo) 62*, 558.

Polymerization of Actin and Actin-like Systems: Evaluation of the Time Course of Polymerization in Relation to the Mechanism†

Carl Frieden* and Dean W. Goddette

ABSTRACT: The time course of protein polymerization of the nucleation–elongation type is examined by using a general computer-simulation solution. For a simple nucleation–elongation scheme, it is shown that the half-time of polymerization is not necessarily a good measure of the nucleus size as has been previously suggested [Oosawa, F., & Kasai, M. (1962) *J. Mol. Biol. 4*, 10–21] since, depending on the mechanism, the apparent nucleus size, measured by a ratio of half-times at two actin concentrations, may be either larger or smaller than the real size. Steady-state equations developed by Wegner and Engel [Wegner, A., & Engel, J. (1975) *Biophys. Chem. 3*, 215–225] present a good description of the time course of polymerization although they are somewhat inflexible with regard to allowing for different mechanisms. Some of the assumptions implicit in the development of these equations are discussed in terms of the effect of changing individual rate constants or dissociation constants on the time course of polymerization. In addition, these steady-state equations have been expanded to include the consequences of a reversible first-order conformational change prior to polymerization. It is shown that a conformational change as a prerequisite to polymerization lengthens the lag time of polymerization and, depending on the conditions, may slow the rate of polymerization. The question of fragmentation and of reannealling is examined, and it is noted that simple relationships to describe these processes may not be possible. It is also shown that studies of the mechanism of polymerization require that a wide range of protein concentrations be used since data over a 2-fold concentration range can easily be fit by at least two different mechanisms. Experimental data for the polymerization of actin which demonstrate some of these points are given.

The mechanism of polymerization of actin or similar proteins has been the subject of considerable interest for a number of years (Oosawa & Kasai, 1962; Oosawa & Arakura, 1975; Korn, 1982; Wegner & Engel, 1975; Arisaka et al., 1975; Pollard & Craig, 1982). It is now generally agreed that actin and some other proteins (i.e., tubulin, bacterial flagellin) polymerize by a nucleation–elongation process in which the formation of a seed nucleus is an unfavorable process, but elongation, by monomer addition to this nucleus, is highly cooperative. While this is the overall mechanism, the specific details for the process of polymerization remain unclear. However, the specific mechanism for this type of process is of considerable interest. For example, the recognition that actin is present in nonmuscle cells as well as muscle cells has intensified interest in the polymerization–depolymerization reaction since it is believed that the process may be important in various cellular functions as well as defining the nature of the cytoskeletal structure or membrane–cytoskeletal interactions (Clark & Spudich, 1977).

General equations (Oosawa & Kasai, 1962; Wagner & Engel, 1975) have been derived for describing nucleation–elongation processes. More recently, we have developed a generalized kinetic simulation system (Barshop et al., 1983) which solves differential equations by numerical integration. We show here that this system can be used to stimulate the full time course of polymerization. Using this system, we will examine the validity of the derived equations developed previously and extend the treatment of the full time course of polymerization to include other factors as well as to questions relating to rate-limiting steps. We conclude that computer simulation of the full time course is a more satisfactory method of relating the kinetic properties of a polymerizing system to possible mechanisms.

Central to relating kinetic properties of polymerization to the mechanism is the ability to quantitatively measure the incorporation of monomer into polymer. For actin, such measurements are best carried out by using fluorescent probes which do not interfere with the polymerization process (Tellam & Frieden, 1982; Cooper et al., 1983b; Tait & Frieden, 1982a; Detmers et al., 1981). Light-scattering methods have also been used (Wegner, 1982; Wegner & Savko, 1982), but these may not be as sensitive. For tubulin incorporation into microtubules, many investigators use the change in absorbance due to turbidity. However, this method may not be a quantitative measure of polymerization since there may be a variety of macromolecular structures formed which scatter light differently (Correia & Williams, 1983). For this reason, the relation of the kinetics of polymerization to the mechanism is best examined by using the polymerization of actin. Ex-

† From the Department of Biological Chemistry, Division of Biology and Biomedical Sciences, Washington University School of Medicine, St. Louis, Missouri 63110. *Received May 20, 1983.* Supported by National Institutes of Health Grant AM 13332.

0006-2960/83/0422-5836$01.50/0

perimental data are presented for actin polymerization which illustrate some of the relationships between the kinetic properties and the mechanism.

Materials and Methods

Rabbit skeletal muscle G-actin was isolated and purified according to Spudich & Watt (1971) with additional gel filtration on Sephadex G-150 (McLean-Fletcher & Pollard, 1980). The actin was stored at −20 °C after lyophilization in the presence of sucrose (2 mg/mg of actin). Lyophilized actin was dialyzed at 4 °C for 16–24 h against 2 mM tris(hydroxymethyl)aminomethane hydrochloride (Tris-HCl), pH 8, containing 200 μM ATP, 50 μM $MgSO_4$, 1.5 mM NaN_3, and 200 μM dithiothreitol or against 2 mM imidazole, pH 7, containing 200 μM ATP, 50 μM $MgSO_4$, 1.5 mM NaN_3, and 1 mM dithiothreitol. This actin is Ca^{2+} free. The protein concentration was determined spectrophotometrically by using $E^{1mg/mL} = 0.63$ at 290 nm (Houk & Ue, 1974).

Before being used, all actin solutions were centrifuged at 180000*g* for 30 min or at 100000*g* for 60 min. Polymerization was followed continuously by measuring the enhancement of actin labeled with *N*-(1-pyrenyl)iodoacetamide, prepared as described by Kouyama & Mihashi (1981). Only trace amounts of the fluorescently labeled actin were used, and the method has been shown to be a measure of the incorporation of monomer into polymer (Tellam & Frieden, 1982; Cooper et al., 1983b). Solutions were stirred for only 10 s after Mg^{2+} addition by using a magnetic stirrer in the bottom of the fluorescence cuvette. All polymerization reactions were carried out at 20 °C. The excitation and emission wavelengths were 365 and 386 nm, respectively.

Kinetic Simulation. We have described elsewhere (Barshop et al., 1983) a generalized simulation system which can be used to describe the time course of many different reaction types. One uses the system by writing down the descriptive equation (i.e., A + B ⇌ C, etc.), and the program sets up the relevant differential equations and solves them by numerical integration. While similar systems have been described (Garfinkel et al., 1977), the system used here is highly interactive as well as being relatively machine independent. Information on the system is available on request. The computer simulation system makes no assumptions relative to steady state or rapid equilibrium and therefore is not constrained by these assumptions. The description of the complete polymerization process would be too complex for this system since so many polymerization steps are involved. Therefore, one simplification, as described below, has been involved.

The kinetic equations used in the description of a simple polymerization mechanism are shown in Scheme I. Several

Scheme I

$$A + A \underset{k_{-1}}{\overset{k_1}{\rightleftharpoons}} A_2$$

$$A_2 + A \underset{k_{-2}}{\overset{k_2}{\rightleftharpoons}} A_3$$

$$A_3 + A \underset{k_{-3}}{\overset{k_3}{\rightleftharpoons}} A_4$$

$$A_4 + A \underset{k_{-4}}{\overset{k_4}{\rightleftharpoons}} A_5$$

$$A_5 + A \underset{k_{-5}}{\overset{k_5}{\rightleftharpoons}} A_6$$

$$A_6 + A \underset{k_{-6}}{\overset{k_6}{\rightleftharpoons}} A_p$$

$$A_p + A \underset{k_{-p}}{\overset{k_p}{\rightleftharpoons}} A_p$$

points should be noted about this scheme. First, by appropriately adjusting the rate constants, one can make the polymerization proceed by an isodesmic mechanism (i.e., all rate constants identical) or by a nucleation–elongation mechanism. The nucleus size, n, is defined as the number of monomers in the largest species which is more likely to dissociate than to grow. Second, the rate constants used in this particular scheme (and in other derivations as well) do not differentiate between the two ends of the actin filament. Thus, k_4, for example, represents the sum of two rate constants for monomer binding to the two ends of a tetrameric molecule while k_{-4} represents the sum of two rate constants for a monomer dissociating for the A_5 oligomers. Third, the species A_p serves as a representation of all polymers and contains no information on the length distribution. We find that a certain number of polymerization steps are required. The number chosen in Scheme I (6 steps) appears to be sufficient since the inclusion of more steps (up to 8 or 10) makes no difference in the time course under many different conditions tested. This number of steps is large enough to make the flux through the step prior to the final step, $A_6 + A \rightleftharpoons A_p$, independent of the nucleus size. In this regard, we also set $k_{-6} = 0$ to prevent the level of A_6 from increasing as the concentration of polymer, A_p, increases. Setting k_{-6} equal to zero at this point in the mechanism does not appear to significantly change the flux through the step. Fourth, the simulation system allows many different outputs. Thus, one can obtain the time course of filament formation, the concentration of A_i (where $i = 2$–6), or the disappearance of monomer. For Scheme I, the output used to represent polymer formation is

$$(c_0 - 2A_2 - 3A_3 - 4A_4 - 5A_5)/c_0 \qquad (1)$$

where c_0 is the total actin concentration. Finally, the mechanism may be easily expanded to include other factors. For example, simple fragmentation and reannealling of filaments might be represented by

$$A_p \underset{k_{-f}}{\overset{k_f}{\rightleftharpoons}} 2A_p \qquad (2)$$

while a first-order conformational change prior to the form of actin which polymerizes can be inserted as

$$B \rightleftharpoons A \qquad (3)$$

An initial binding step followed by a conformational change would be represented as

$$B + L \rightleftharpoons BL \rightleftharpoons A \qquad (4)$$

and so on.

Solutions of differential equations such as those given by Wegner & Engel (1975; Wegner, 1982) were obtained by numerical integration using Gear's algorithm (Gear, 1971).

Results and Discussion

Simple Nucleation–Elongation: Oosawa–Kasai Model. The kinetics of polymerization were developed initially for the field of polymer chemistry (Flory, 1953) and were applied to protein systems by Oosawa & Kasai (1962).

In order to obtain a differential equation which could be explicitly integrated, Oosawa and Kasai assumed that certain reverse rate constants in the polymerization process were negligible. The treatment assumes that the apparent forward rate constant for nucleation is in fact the product of a rate constant for an irreversible step leading either to the nucleus or to a species which serves as the nucleus (i.e., an isomerization of the nucleus) and a ratio of rate constants reflecting reversible steps prior to the formation of the nucleus. Thus, for example, in the case where the nucleus is a trimer, k_2 of

Table I: Ratios of Half-Times ($t_{1/2}$) of Polymerization at Two Actin Levels for Different Mechanisms[a]

mechanism	R (=$t_{1/2}$ at 5 μM actin/ $t_{1/2}$ at 20 μM actin)
Oosawa-Kasai model[b] (see text)	8
unfavorable but equal equilibria leading to nucleus[c]	17
unfavorable and unequal equilibria leading to nucleus[d]	$8 < R < 17$
fragmentation or fragmentation plus reannealling[e]	<8
first-order rate process prior to polymerization[f]	≤17

[a] Nucleus size is a trimer. The actual values for the ratios may depend on the rate constants chosen. Those given here are indicative of the trend. [b] Critical concentration set equal to zero. [c] Rate constants given in legend to Figure 2 (top curve). [d] Rate constants given in legend to Figure 2 (bottom curve). [e] Rate constants given in legend to Figure 4. [f] Rate constants given in legend to Figure 7.

Scheme I might be assumed to be the slow step while the formation of A_2 is represented by the relationship $A_2 = A_2k_{-1}/k_1$. With this assumption, and the assumption that the rate constant for disassembly of the polymer is negligible, they obtained

$$\ln \frac{\{1 + [1 - (c_1/c_0)^n]\}^{1/2}}{\{1 - [1 - (c_1/c_0)^n]\}^{1/2}} = 2n^{1/2}(k^*k)^{1/2}c_0^{n/2}t \quad (5)$$

where c_1 is the monomer concentration, c_0 is the total concentration, n is the size of the nucleus in terms of the number of monomers, and k^* and k are the rate constants for nucleus formation and elongation, respectively (Oosawa & Kasai, 1962; Oosawa & Asakura, 1975). Among other characteristics, this equation predicts that the half-time for polymerization ($t_{1/2}$) is inversely proportional to the $n/2$ power of the total concentration. Thus, this model should provide information as to the size of the nuclei. For example, for a 4-fold change in the total actin concentration, an 8-fold change in the $t_{1/2}$ would be predicted for a nucleus size of 3. It should be pointed out that noninteger values of n would indicate that this treatment is incorrect since it should predict only integral values.

Indeed, if the assumptions made are incorporated into the model shown in Scheme I or into one in which the nucleus must undergo an irreversible change prior to elongation, this prediction is verified. This is shown in Table I which compares this model with other mechanisms. As discussed below, other mechanisms do not obey this rule.

Wegner Formulation. Wegner and co-workers (Wegner & Engel, 1975; Wegner, 1982; Wegner & Savko, 1982), using steady-state assumptions, have derived two differential equations which, when solved simultaneously, give the time course of polymerization. The equations used (not including fragmentation which is discussed later) are

$$\frac{dC}{dt} = (kc_1 - k')c_1^n \prod_{i=1}^{n-1} k_i/k_i' \quad (6)$$

and

$$\frac{dc_1}{dt} = -(kc_1 - k')C \quad (7)$$

where C is the molar concentration of filaments, k_i and k_{-i} are rate constants involved in nucleus formation, n is the size of the nucleus, c_1 is the monomer concentration, and k and k' are rate constants for elongation and disassembly of the filament, respectively. For this formulation, the product $\prod_{i=1}^{n-1} k_i/k_i'$ is frequently represented as a single constant, K_n. The implicit assumption is that all rate constants leading to the formation of the nucleus are equal as are all rate constants involving dissociation of the species of nucleus size or smaller. Thus, in Scheme I, the formulation implies that if the nucleus is a trimer then $k_1 = k_2$ and $k_{-1} = k_{-2}$. Similarly, it is implicitly assumed that all elongation steps have identical rate constants as do all disassembly steps (i.e., $k_3 = k_4 = k_5 = k_6 = k_p = k$ and $k_{-3} = k_{-4} = k_{-5} = k_{-6} = k_{-p} = k'$).

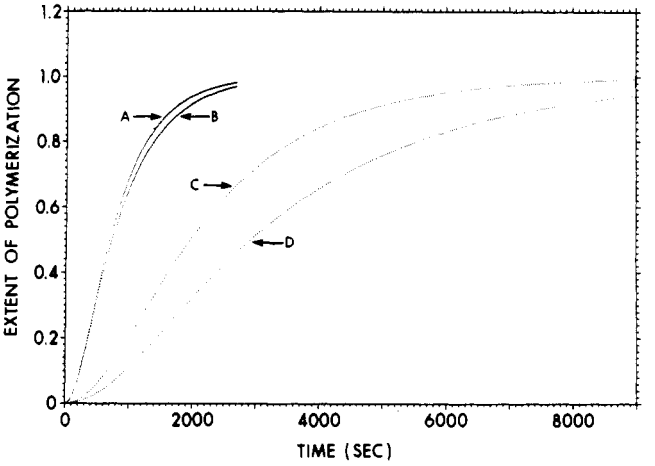

FIGURE 1: Comparison of the full time course of polymerization at two actin levels using the formulation of Oosawa and Kasai and the simulation system shown in Scheme I. The figure shows that $t_{1/2}$ is not necessarily a measure of nucleus size (see text). The nucleus size is assumed to be a trimer. For the Oosawa and Kasai system, $k_2 = 1 \times 10^{-4}$ M^{-1} s^{-1} and $k_{-2} = 0$. For the reversible nucleation system, $k_2 = 1 \times 10^6$ M^{-1} s^{-1} and $k_{-1} = k_{-2} = 2.5 \times 10^5$ s^{-1}. The other rate constants used for both cases are $k_1 = 1 \times 10^6$ M^{-1} s^{-1}, k_3–k_6 and $k_p = 1 \times 10^6$ M^{-1} s^{-1}, and k_{-3}–k_{-6} and $k_{-p} = 0$. Curves A and C are the time courses obtained at 20 and 10 μM actin concentrations, respectively, for the Oosawa and Kasai model while curves B and D are those for reversible nucleation of all steps leading to the nucleus. The time courses at different actin concentrations are normalized to the same extent of polymerization.

With reversibility of all steps involved in polymerization, the predictions of eq 5 are no longer correct. Table I shows that the ratio of half-times over a 4-fold actin concentration for the case of a trimer nucleus with $k_{-1}/k_1 = k_{-2}/k_2 = 17$ rather than 8. The apparent nucleus size according to eq 5 would be about 4 rather than the actual value of 3 (a trimer). In terms of the experimental results, the dependence of the half-time of polymerization on the actin concentration is larger than expected. Stated in another way, the apparent nucleus size calculated from the $t_{1/2}$ values is larger than the actual size. Figure 1 shows simulated data to illustrate this point for a nucleus size assumed to be a trimer. Curves A and C represent the time course of polymerization assuming irreversibility of trimer formation at two actin levels while curves B and D represent reversible trimer formation at the two actin concentrations. The rate constants (listed in the legend) where chosen to give approximately the same time course at the higher actin concentration. Larger differences in the ratio of half-times for polymerization occur for larger nucleus sizes (not shown). Thus, the use of the ratio of half-times of polymerization at different actin concentrations as a measure of nucleus size is questionable.[1]

[1] It should be noted that if there are two or more slow irreversible steps leading to the nucleus, the prediction for $t_{1/2}$ given by eq 5 will not hold at all. Similarly, if trimer or tetramer formation is a multicollison event (i.e., $3A \rightleftharpoons A_3$), the formulation breaks down as well.

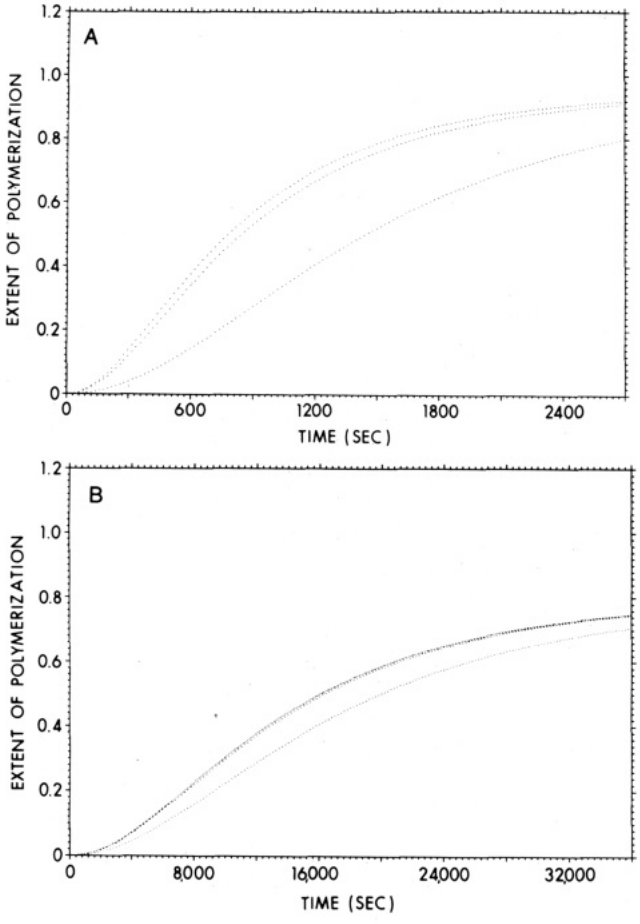

FIGURE 2: Effect of unequal equilibrium constants for dimer and trimer formation on the time course of polymerization. In panel A, the actin concentration is 20 μM. In panel B, the actin concentration is 5 μM. The following rate constants were used (see Scheme I): (top curve) $k_{-1} = k_{-2} = 2 \times 10^5$ s^{-1}; (middle curve) $k_{-1} = 4 \times 10^8$ s^{-1}, $k_{-2} = 100$ s^{-1}; (lower curve) $k_{-1} = 100$ s^{-1}, $k_{-2} = 4 \times 10^8$ s^{-1}. These correspond to values of $\prod k_i/k_i' (=K_n)$ of 25 M^{-2} in each case. Other rate constants in all cases were as follows: k_1–k_6 and $k_p = 1 \times 10^6$ M^{-1} s^{-1}, k_{-3}–k_{-5} and $k_{-p} = 1$ s^{-1} ($k_{-6} = 0$, see Materials and Methods).

As stated previously, those rate constants involved in nucleus formation, i.e., $\prod_{i=1}^{n-1} k_i/k_i'$, are collected as the term K_n. Thus, for a nucleus the size of a trimer, there is no distinction between the dissociation constants for dimer and trimer formation. Over a very wide range of dissociation constants, this assumption appears to be satisfactory. Figure 2 shows, however, that it does break down if the dissociation constants for dimer and trimer formation are sufficiently disparate. In Figure 2, $K_n = 25$ M^{-2} ($k_1/k_{-1} = k_2/k_{-2} = 5$ M^{-1}). Changes in the time course of polymerization do not become obvious until the difference in k_{-1}/k_1 and k_{-2}/k_2 is on the order of 10^6. In this case, surprisingly, the dependence of the polymerization time course as a function of protein concentration may appear to be less than expected for the fully reversible case. For the case where the formation of trimer becomes more favorable relative to that of dimer, the result approaches, in the limit, a nucleus size of 2 rather than 3. This is demonstrated in Figure 3. Here are shown data for the polymerization of actin at two levels of actin concentration (23.5 and 5.7 μM). The curve on the left is the superimposition of three curves which reflect real data and the fit of the data by simulation using either a dimer or a trimer as the nucleus. The curves to the right show the expected time course using a dimer or a trimer as the nucleus compared to the real data. Clearly, the real data fall between the simulations of dimer and trimer nuclei.

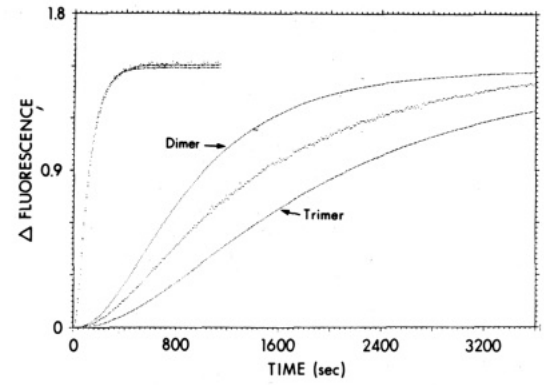

FIGURE 3: Simulation of actin polymerization assuming either a dimer or a trimer as nucleus. The left-most curve is the superimposition of three curves which include experimental data (actin concentration 23.5 μM, pH 8 and 20 °C) and two simulated curves determined by using Scheme I. The value of $\prod_{i=1}^{n-1} k_i/k_i' (=K_n)$ is 0.0167 M^{-1} for the dimer and 730 M^{-2} for the trimer. The right-most curves labeled dimer and trimer are the expected time courses of polymerization at 5.7 μM actin with the rate constants with either a dimer or a trimer as the nucleus. The experimental data fall between the dimer and trimer curves. Other rate constants used (k_3–k_p, k_{-3}–k_{-p}) are given in the legend to Figure 2.

The most likely explanation for this result is that the formation of dimer is much less favorable than that of trimer, and this explanation has been used elsewhere to describe data of this kind (Frieden, 1983).

The point is also shown in Table I. The experimental consequence of this result is that the apparent nucleus size, as measured by $t_{1/2}$ values, will be smaller than the real value.

The second major assumption in all formulations is that once the nucleus is formed all rate constants for elongation (or dissociation of the monomer from the filament) are identical. Unfortunately, this gives little information as to what may be the rate-limiting step in the elongation process. With very unfavorable equilibria leading to the formation of the nucleus, a critical step in the rate of polymerization is the first elongation step (which we can call k_{i+1}). Changes in the rate constants for subsequent intermediate steps in elongation are not nearly so effective in changing the overall time course of polymerization as changing the value of k_{i+1}. For a given nucleus size, an empirical observation is that when the ratio $k_{i+1}k_p/k_{-p}$ is constant, the time course of the polymerization remains the same. (As before, k_{i+1} represents the forward rate constant from the viable nucleus, and k_p and k_{-p} are defined in Scheme I.) When the equilibria leading to the nuclei are quite different (as shown by Figure 2, for example), the critical rate constant may be either k_{i+1} or the forward rate constant directly preceding it.

Extensions to the Simple Nucleation–Elongation Mechanisms: Fragmentation and Reannealling. In more recent publications (Wegner, 1982; Wegner & Savko, 1982; Cooper et al., 1983a), investigators have included a term to represent the irreversible fragmentation of actin filaments, thereby creating more filament ends from which elongation may occur. This process has been used to explain data obtained by Wegner & Savko (1982) and by Cooper et al. (1983a), although other investigators have performed experiments under conditions in which the term does not appear to be necessary (Tobacman & Korn, 1983; Frieden, 1983). We have observed that reannealling of sheared filaments is a reasonably rapid process (Tait & Frieden, 1982a). Thus, fragmentation is probably reversible, and it is possible that under some conditions reannealling may be rapid enough so that the fragmentation term is not apparent.

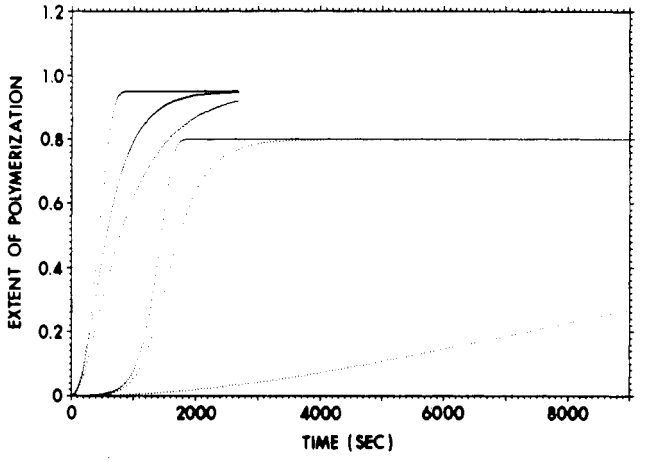

FIGURE 4: Effect of fragmentation with and without reannealling on the time course of polymerization. The three curves on the left side of the figure are at a protein concentration of 20 μM while the three on the right side are at 5 μM. In each set of three, the left-most curve shows fragmentation alone, the middle curve shows fragmentation plus reannealling, and the right curve is the time course under the same conditions with no fragmentation or reannealling. Rate constants used are those given for the top curve in the legend of Figure 2, and with k_f and $k_{-f} = 0.005\ s^{-1}$ and $2 \times 10^6\ M^{-1}\ s^{-1}$, respectively (see eq 2 or 9).

One equation used for irreversible fragmentation (Wegner, 1982) is an extension of eq 6:

$$\frac{dC}{dt} = (kc_1 - k')c_1^n \prod_{i=1}^{n-1} k_i/k_i' + k_f C \qquad (8)$$

where k_f is the fragmentation rate constant and C, as before, is the molar concentration of filaments. Since reannealling is a second-order process, while fragmentation is a first-order process, it is not correct to consider that k_f is the sum of the fragmentation and reannealling processes. Thus, the proper equation, in Wegner's terminology, would be

$$\frac{dC}{dt} = (kc_1 - k')c_1^n \prod_{i=1}^{n-1} k_i/k_i' + k_f C - k_{-f}C^2 \qquad (9)$$

where k_{-f} would be the reannealling rate constant.[2] The inclusion of this term can change the shape of the time course of polymerization.

This is shown by Figure 4, which illustrates the effect of fragmentation alone and fragmentation plus reannealling according to eq 8 and 9 at two different protein concentrations (shown by two sets of three curves each). In each set (i.e., at each protein concentration), the right-most curve is without fragmentation, the left-most curve is with fragmentation, and the middle curve is with fragmentation and reannealling.[3] Three points should be noted. First, the effect of fragmentation is much greater at the lower protein concentration (5 μM in this case) than at the higher one (20 μM). Second, for a given rate constant of reannealling, the effect is larger at the higher protein concentration than at the lower concentration. As stated above, this results from the fact that reannealling is a second-order process. Third and most important is that if reannealling occurs and is not included in the data fitting as a function of protein concentration, the wrong value for the nucleus size is likely to be found, with the apparent value being lower than the real value (also see Table I).

Figure 5 shows data for actin polymerization which may illustrate this point. Data were obtained under the same conditions at two actin concentrations (5.7 and 23.5 μM) at pH 7 and at pH 8 and 20 °C. At the high actin concentration, the time course of polymerization is approximately the same at both pH values. However, at the low concentration, polymerization at pH 7 is much more rapid than that at pH 8. Comparison with Figure 4 shows that this is the expected behavior if fragmentation were an important component of the time course. We have shown elsewhere (Frieden, 1983) that no fragmentation term is needed to explain the pH 8 data. The most likely explanation for the data shown in Figure 5 is that at pH 7 fragmentation (or fragmentation and reannealling) occurs.

For small protein filaments in which there is no network formation or fragmentation, a reannealling term ($k_{-f}C^2$ of eq 9) would result in a slower time course most noticeable toward the end of the polymerization as a consequence of a decrease in the filament ends which can serve as elongation points. In this case, the time course becomes

$$\frac{dC}{dt} = (kc_1 - k')c_1^n \prod_{i=1}^{n-1} k_i/k_i' - k_{-f}C^2 \qquad (10)$$

Cooper et al. (1983a) have included a fragmentation term to describe polymerization induced by KCl and Ca^{2+}, which is different from that shown by eq 8. They attempt to relate the degree of fragmentation to the length of the polymer, instead of polymer concentration, by using the fragmentation term $FN(P/N)^2$ where N is the polymer number concentration, F is a fragment factor, and P is the weight concentration of polymer (moles of actin monomer incorporated into polymer). While it is probably correct that fragmentation is a function of filament length, the exact dependence may be quite difficult to formulate. Cooper et al. (1983a) have used the term described above because it appears to best fit the experimental data, although it should be noted that they did not consider the possibility of reannealling. A formulation which would consider filament length should actually be of the form $\sum_{j=n}^{\infty} k_j C_j$ where j represents each filament species of different length. If the distribution of filament lengths is reasonably constant over some period of time during polymerization, it may be appropriate to replace the summation term with $k_f C$ which is the term used in eq 8 and 9. The data of Kondo & Ishiwata (1976) indicate rather similar distributions of the length of actin filaments over short time periods.

As with reannealling (see footnote 2), fragmentation may also be a function of the network structure, and in the presence of extensive cross-linking, which occurs at various times in polymerization (Tait & Frieden, 1982c), fragmentation would be decreased. It seems clear at this point that it may be difficult to describe fragmentation, as well as reannealling, by simple relationships.

Inclusion of an Activation Step Prior to Polymerization. For a reversible first-order activation step, Scheme I is expanded to Scheme II.

[2] In F-actin solutions, it is clear that the filaments become cross-linked as polymerization proceeds (Tait & Frieden, 1982c). In networks of F-actin, the reannealling process may not be one expected for the simple diffusion of two ends to form a longer filament. Thus, one filament end formed by fragmentation may be held rigidly by the nature of the gel while the other may move around near it in a restricted way. Thus, the expression given in eq 9 may no longer be correct since the rate of reannealling may be between first and second order and the order may change as polymerization proceeds and networks form. This is an interesting problem which needs further examination.

[3] The value of the reannealling rate constant is probably larger than might be expected but was chosen for illustration purposes only.

Scheme II

$$B \underset{k_{-a}}{\overset{k_a}{\rightleftharpoons}} A$$

$$A + A \underset{k_{-1}}{\overset{k_1}{\rightleftharpoons}} A_2$$

$$A_2 + A \underset{k_{-2}}{\overset{k_2}{\rightleftharpoons}} A_3$$

$$\vdots$$

$$A_p + A \underset{k_{-p}}{\overset{k_p}{\rightleftharpoons}} A_p$$

In terms of the Wegner formulation, three differential equations are required. These are

$$\frac{dB}{dt} = -k_a B + k_{-a} A \tag{11}$$

$$\frac{dA}{dt} = k_a B - k_{-a} A - (kA - k')C \tag{12}$$

$$\frac{dC}{dt} = (kA - k')A^n \prod_{i=1}^{n-1} k_i/k_i' \tag{13}$$

where the polymerization time course (i.e., the disappearance of monomer into polymer) is represented by $c_0 - A - B$, c_0 being the total protein concentration, and c_1 in previous equations is replaced by A, the concentration of the polymerizable species. These equations are different from those presented by Tobacman & Korn (1983) for an irreversible activation step.

For the polymerization of actin, a reversible first-order conformational change as a prerequisite to polymerization (as shown in Scheme II) has also been proposed by Rouayrenc & Travers (1981) while Cooper et al. (1983a) suggested that activation is rate limiting for nucleus formation. These latter authors have used steady-state assumptions similar to those used in developing eq 11–13 to describe experimental data in the presence of Mg^{2+} and KCl.

We have recently shown (Frieden, 1983) that an activation step in the Mg^{2+}-induced polymerization of actin is a step identical with the conformational change induced by Mg^{2+} when binding to the tight metal binding site (Frieden et al., 1980; Frieden, 1982). This site binds either Ca^{2+} somewhat tighter than Mg^{2+} (Frieden, 1982), and consequently, Ca^{2+} can effectively decrease the rate of the Mg^{2+}-induced conformational change.

It should be noted that the formulation of $B \rightleftharpoons A$ to represent the ligand binding followed by a conformational change (such as the Mg^{2+}-induced conformational change in G-actin) is not formally correct. Rather, this should be

$$B + Mg^{2+} \underset{}{\overset{K_m}{\rightleftharpoons}} BMg \rightleftharpoons A$$

However, if the first step represents poor binding followed by a conformational change in which the overall binding is tight, the $B \rightleftharpoons A$ formulation is adequate. In fact, this appears to be the case for Mg^{2+} binding to actin since the first dissociation constant, K_m, is about 1 mM under normal conditions while the overall dissociation constant for Mg^{2+} binding is about 40 μM (Frieden, 1982).

A slow reversible first-order process can have an effect both on the lag time and on the maximum rate of polymerization. The lag time is a consequence of both the unfavorable formation of nuclei as well as the rate of the conformational change. However, the contribution of these two effects to the lag time will depend on the rate of the polymerization reaction.

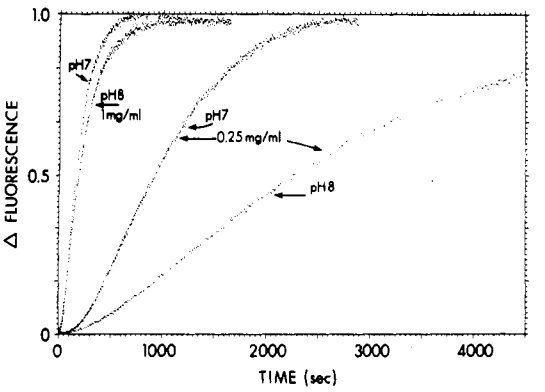

FIGURE 5: Comparison of actin polymerization at two pH values and two concentrations. Actin polymerization was initiated by the addition of 2 mM Mg^{2+}. At pH 7, the buffer was 2 mM imidazole while at pH 8 the buffer was 2 mM Tris-HCl. Other experimental conditions are as given under Materials and Methods. As discussed in the text, the data may be evidence for fragmentation at pH 7 relative to that at pH 8.

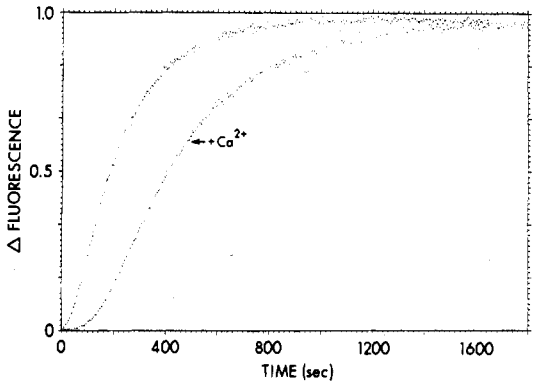

FIGURE 6: Mg^{2+}-induced polymerization of G-actin in the presence and absence of Ca^{2+}. Actin (23.5 μM) was polymerized by the addition of 2 mM Mg^{2+} at 20 °C in 2 mM Tris-HCl buffer at pH 8. Polymerization was followed by fluorescence, and other experimental conditions are as described under Materials and Methods. The Ca^{2+} concentration used was 400 μM in the curve at the right.

Thus, at very slow rates of polymerization, the conformational change may not contribute appreciably to the lag time while at very fast rates of polymerization, the lag time may be primarily a consequence of the conformational change. Similarly, the maximum rate of polymerization can depend on the rate of the conformational change since the important variable in determining this rate is the concentration of the species after the conformational change but prior to polymerization. If the polymerization rate is rapid, the concentration of this species may be low because of the slow rate leading to it (the conformational change) and the fast rate leading away from it (either nucleation or elongation). At slow rates of polymerization, these effects are not as important.

An example of the effect of slowing the rate of a reversible conformational change on the polymerization kinetics is shown in Figure 6. Here are shown data for the Mg^{2+}-induced polymerization of actin in the presence and absence of Ca^{2+}. As discussed above, Ca^{2+} effectively decreases the rate of a Mg^{2+}-induced conformational change essential for polymerization (Frieden, 1983). As a consequence, the lag time is increased, and the rate of polymerization is decreased.

Importance of Using a Wide Range of Actin Concentrations. Several studies in which the full time course of polymerization has been analyzed have used rather narrow ranges of actin concentrations (i.e., about 2-fold). It is important, however, to use a range of actin concentrations which is quite broad (i.e., 5–6-fold), since a narrow range may not distinguish between

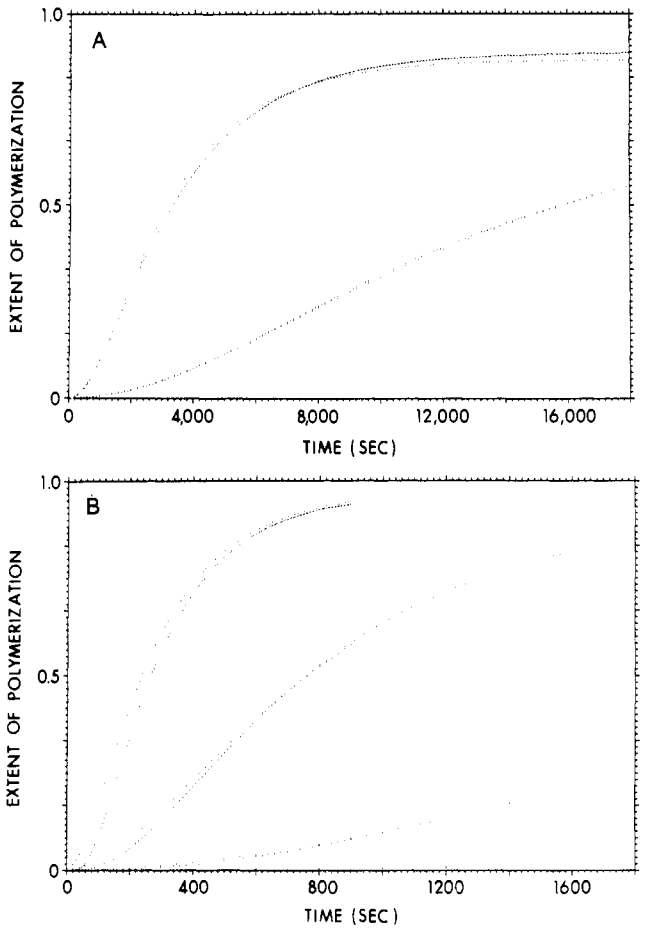

FIGURE 7: Demonstration that over a limited range of actin concentrations two different mechanisms fit the same data. The two mechanisms are those shown in Schemes I and II where the latter requires a first-order activation step prior to polymerization. Panel A shows the full time course at 5 and 10 μM actin; panel B is the full time course at 10, 20, and 35 μM actin. In both panels, the rate constants are k_1–k_6 and $k_p = 1 \times 10^6$ M^{-1} s^{-1}, $k_1 = 1.2 \times 10^5$ s^{-1}, $k_{-2} = 1.1 \times 10^5$ s^{-1}, and k_{-3}–k_{-5} and $k_{-p} = 1$ s^{-1} ($k_{-6} = 0$). For curves plotted according to Scheme II, $k_a = 0.05$ s^{-1} and $k_{-a} = 0.01$ s^{-1}. In panel B, the curves which show the greater lag are those plotted according to Scheme II.

mechanisms. Figure 7 demonstrates this point. In this case, we have used the system shown in Scheme II (that is, a required first-order activation step) but fit the data with the mechanism which is shown in Scheme I. Examination of the figure shows that over a 2-fold range of actin concentrations (5 and 10 μM actin), the fit of the two mechanisms is reasonably close (Figure 7A). However, as shown in Figure 7B, the fit fails at higher actin concentrations (20 and 35 μM). Although we have not tested the comparison of other mechanisms in the same way, it seems quite likely that one could generate similar results. Investigators are, therefore, urged to use as wide a range of actin concentrations as possible.

Conclusions

We have tested the validity of various mechanisms (and related differential equations) used to fit the full time course of polymerization of proteins which proceed, in general, by an nucleation–elongation mechanism. Such an examination seems warranted because of the recent development in quantitative measures of the process in unperturbed systems. Examination of the models discussed here indicates that there is no simple measure (i.e., half-time, lag time) which would characterize the rate of polymerization. Use of the ratio of half-times of polymerization at different protein concentrations may not be a good measure of the nucleus size or an indication of the mechanism of polymerization. Thus, it is necessary to be able to fit the full time course of the polymerization. Some of the equations currently in use are adequate for simple polymerization processes but inadequate for more complex, and probably more realistic, systems. In the present paper, existing mechanisms have been expanded to include a step involving activation of monomer prior to polymerization and the consequences of a filament fragmentation step being reversible (reannealling). Additional changes in the mechanism are discussed. Aspects of protein polymerization, such as differential growth from the two ends of the filament, are not discussed but could be included within the context of the mechanisms presented. The use of a wide range of protein concentrations in the determination of the mechanism is stressed.

Acknowledgments

We thank Dr. Bruce Barshop for setting up the initial computer programs needed to solve the equations used in this paper. Helen Gilbert and Derek Lazard provided excellent technical assistance.

References

Arisaka, F., Noda, H., & Maruyama, K. (1975) *Biochim. Biophys. Acta 400*, 263–274.

Barshop, B. A., Wrenn, R. F., & Frieden, C. (1983) *Anal. Biochem. 130*, 134–145.

Clark, M., & Spudich, J. (1977) *Annu. Rev. Biochem. 66*, 797–822.

Cooper, J. A., Buhle, E. C., Jr., Walker, S. B., Tsong, T. Y., & Pollard, T. D. (1983a) *Biochemistry 22*, 2193–2202.

Cooper, J. A., Walker, S. B., & Pollard, T. D. (1983b) *J. Muscle Res. Cell Motil. 4*, 253–262.

Correia, J. J., & Williams, R. C., Jr. (1983) *Annu. Rev. Biophys. Bioeng. 12*, 211–235.

Detmers, P., Weber, A., Elzinga, M., & Stephens, R. E. (1981) *J. Biol. Chem. 256*, 99–105.

Flory, P. J. (1953) in *Principles of Polymer Chemistry*, Cornell University Press, Ithaca, NY.

Frieden, C. (1982) *J. Biol. Chem. 257*, 2882–2886.

Frieden, C. (1983) *Proc. Natl. Acad. Sci. U.S.A.* (in press).

Frieden, C., Lieberman, D., & Gilbert, H. R. (1980) *J. Biol. Chem. 255*, 8991–8993.

Garfinkel, L., Kohn, M. C., & Garfinkel, D. (1977) *CRC Crit. Rev. Bioeng. 2*, 329–361.

Gear, C. W. (1971) *Commun. ACM 14*, 176–179.

Houk, T. W., Jr., & Ue, K. (1974) *Anal. Biochem. 62*, 66–74.

Kondo, H., & Ishiwata, S. (1976) *J. Biochem. (Tokyo) 79*, 159–171.

Korn, E. D. (1982) *Physiol. Rev. 62*, 672–737.

Kouyama, T., & Mihashi, K. (1981) *Eur. J. Biochem. 114*, 33–38.

MacLean-Fletcher, S., & Pollard, T. D. (1980) *Biochem. Biophys. Res. Commun. 96*, 18–27.

Oosawa, F., & Kasai, M. (1962) *J. Mol. Biol. 4*, 10–21.

Oosawa, F., & Asakura, S. (1975) in *Thermodynamics of the Polymerization of Protein*, Chapter 4, Academic Press, New York.

Pollard, T. D., & Craig, S. W. (1982) *Trends Biochem. Sci. (Pers. Ed.) 7*, 55–58.

Rouayrenc, J., & Travers, F. (1981) *Eur. J. Biochem. 116*, 73–77.
Spudich, J. A., & Watt, S. (1971) *J. Biol. Chem. 246*, 4866–4871.
Tait, J. F., & Frieden, C. (1982a) *Arch. Biochem. Biophys. 216*, 133–141.
Tait, J. F., & Frieden, C. (1982b) *Biochemistry 21*, 6046–6053.
Tait, J. F., & Frieden, C. (1982c) *Biochemistry 21*, 3666–3674.
Tellam, R., & Frieden, C. (1982) *Biochemistry 21*, 3207–3214.
Tobacman, L. S., & Korn, E. D. (1983) *J. Biol. Chem. 258*, 3207–3214.
Wegner, A. (1982) *Nature (London) 296*, 200–201.
Wegner, A., & Engle, J. (1975) *Biophys. Chem. 3*, 215–225.
Wegner, A., & Savko, P. (1982) *Biochemistry 21*, 1909–1913.

Location of an Essential Carboxyl Group along the Heavy Chain of Cardiac and Skeletal Myosin Subfragments 1†

Marie Körner,* Nguyen Van Thiem, Robert Cardinaud,‡ and Gabrielle Lacombe

ABSTRACT: Cardiac and skeletal myosin subfragments 1 cleaved into three fragments were modified by 1-cyclohexyl-3-(2-morpholinoethyl)carbodiimide metho-*p*-toluenesulfonate in the presence of the nucleophile nitrotyrosine ethyl ester. The effects observed (first-order kinetics of ATPase inactivation, incorporation of 1 mol of nitrotyrosine/mol of subfragment 1) were similar to those previously observed for the nondigested subfragments 1 [Lacombe, G., Van Thiem, N., & Swynghedauw, B. (1981) *Biochemistry 20*, 3648–3653; Körner, M., Van Thiem, N., Lacombe, G., &Swynghedauw, B. (1982) *Biochem. Biophys. Res. Commun. 105*, 1198–1207]. For both native and digested subfragments 1, which were inactivated to the extent of about 70%, the location of the label nitrotyrosine was performed by immunological blotting with ^{125}I-labeled anti-nitrotyrosine immunoglobulins. It was found that the modified residue was essentially located on the heavy chain for the native subfragments 1 and on the 50K peptide for the digested subfragments 1.

In recent years, a number of studies have been devoted to the structure–function relationship of myosin, an oligomeric enzyme consisting of two heavy chains and four light chains. The latter have been shown by several workers to play a role in the regulation of the myosin–actin interaction [see reviews by Taylor (1979) and Adelstein & Eisenberg (1980)]. For the heavy chains, the two important functions of myosin, adenosine 5′-triphosphate (ATP)[1] hydrolysis and actin activation, have recently been attributed to the isolated heavy chain (Maruta et al., 1978; Wagner & Giniger, 1981; Sivaramakrishnan & Burke, 1982). However, the chemical structure of the catalytic site of myosin is unknown, although a number of amino acid residues have long been suggested as being essential (cysteine, lysine, arginine, histidine, tyrosine). Some functional groups have been located, due to the fact that controlled fragmentation of the myosin head which contains the ATPase and the actin-binding sites produced three positioned peptides: 27K–50K–20K (Balint et al., 1978; Mornet et al., 1979; Yamamoto & Sekine, 1979a; Cardinaud, 1979). This is the case for the reactive lysyl residue located in the 27K domain (Mornet et al., 1980; Hozumi & Mühlrad, 1981; Miyanishi & Tonomura, 1981), the SH_1 and SH_2 cysteinyl residues in the 20K domain (Cardinaud, 1979; Walser et al., 1981; Sutoh, 1981), and the actin-binding sites in the 50K and 20K peptides (Mornet et al., 1981a; Yamamoto & Sekine, 1979b; Sutoh, 1982).

In previous studies (Lacombe et al., 1981; Körner et al., 1982), we showed that, through carbodimide modification, skeletal and cardiac myosin subfragments 1 incorporated 1 mol of nucleophile (nitrotyrosine) per mol of S1, resulting in a complete loss of ATPase activity. These results suggested the involvement of one carboxyl residue. As preliminary experiments using the ^{14}C-labeled nucleophile were not satisfactory, the location of this residue was carried out by an immunodetection procedure. For this, antibodies specific to the marker (nitrotyrosine) were prepared and used as probes in immunoblots of S1 fragments obtained with digestion by trypsin. These studies were carried out in parallel on cardiac and skeletal myosins. In both myosins, the modified residue was found essentially on the heavy chain in the case of native S1 and on the 50K peptide in the case of fragmented S1.

Materials and Methods

Chemicals. CNBr-activated Sepharose 4B was purchased from Pharmacia. 1-Cyclohexyl-3-(2-morpholinoethyl)carbodiimide metho-*p*-toluenesulfonate, 1-ethyl-3-[3-(dimethylamino)propyl]carbodiimide, nitrotyrosine ethyl ester, and bovine γ-globulin were purchased from Fluka. [^{14}C]Nitrotyrosine ethyl ester was prepared by Le Service des Molécules Marquées, Commissariat ã l'Energie Atomique, Saclay, France. 3-Nitro-L-tyrosine was an ICN Pharmaceuticals product. Bovine serum albumin and soybean trypsin inhibitor were purchased from Calbiochem. TPCK–trypsin and α-

† From Inserm U 127, Hopital Lariboisière, Paris 75010, France. *Received December 27, 1982.* This investigation was supported by Grant 805034 from the Institut National de la Santē et de la Recherche Mēdicale.

‡ Present address: Dēpartement de Biologie, Centre d'Etudes Nucléaires de Saclay, Gif-sur-Yvette, France.

[1] Abbreviations: S1, α-chymotryptic myosin subfragment 1; CMC, 1-cyclohexyl-3-(2-morpholinoethyl)carbodiimide metho-*p*-toluenesulfonate; NTEE, 3-nitro-L-tyrosine ethyl ester; EDTA, ethylenediaminetetraacetic acid; ATP, adenosine 5′-triphosphate; ADP, adenosine 5′-diphosphate; Tris, tris(hydroxymethyl)aminomethane; $NaDodSO_4$, sodium dodecyl sulfate; TPCK, tosylphenylalanyl chloromethyl ketone.

0006-2960/83/0422-5843$01.50/0